

# **Wildfire influences on the variability and trend of summer surface ozone in the mountainous western United States**

Xiao Lu<sup>1</sup>, Lin Zhang<sup>1</sup>, Xu Yue<sup>2</sup>, Jiachen Zhang<sup>3</sup>, Daniel A. Jaffe<sup>4</sup>, Andreas Stohl<sup>5</sup>, Yuanhong Zhao<sup>1</sup>,  
5 Jingyuan Shao<sup>1</sup>

<sup>1</sup>Laboratory for Climate and Ocean-Atmosphere Sciences, Department of Atmospheric and Oceanic  
Sciences, School of Physics, Peking University, Beijing 100871, China

<sup>2</sup>School of Forestry and Environmental Studies, Yale University, New Haven, Connecticut 06511,  
10 USA

<sup>3</sup>Department of Civil and Environmental Engineering, Viterbi School of Engineering, University of  
Southern California, Los Angeles, CA 90089, USA

<sup>4</sup>School of Science, Technology, Engineering and Math, University of Washington Bothell WA and  
Department of Atmospheric Sciences, Seattle WA 98011, USA

15 <sup>5</sup>Norwegian Institute for Air Research, 2007 Kjeller, Norway

*Correspondence to:* Lin Zhang (zhanglg@pku.edu.cn)

20 **Abstract.** Increasing wildfire activities in the mountainous western US may present a challenge for the region to attain a recently revised ozone air quality standard in summer. Using current Eulerian chemical transport models to examine the wildfire ozone influences is difficult due to uncertainties in fire emissions, inadequate model chemistry and resolution. Here we quantify the wildfire influence on the ozone variability, trends, and number of high MDA8 (daily maximum 8-h average) ozone days  
25 over this region in summers (June, July and August) 1989-2010 using a new approach. We define a Fire Index using retroplumes (plumes of back-trajectory particles) computed by a Lagrangian dispersion model (FLEXPART), and develop statistical models based on the Fire Index and meteorological parameters to interpret MDA8 ozone concentrations measured at 13 Intermountain West surface sites. We show that the statistical models are able to capture the ozone enhancements by  
30 wildfires and give results with some features different from the GEOS-Chem Eulerian chemical transport model. Wildfires enhance the Intermountain West regional summer mean MDA8 ozone by 0.3-1.5 ppbv (daily episodic enhancements reach 10-20 ppbv at individual sites) with large interannual variability, which are strongly correlated with the total MDA8 ozone. We find large fire impacts on the number of exceedance days; for the 13 CASTNet sites, 31% of the summer days with MDA8 ozone  
35 exceeding 70 ppbv would not occur in the absence of wildfires.

## 1 Introduction

Ozone is a secondary air pollutant that exerts negative effects on human health and vegetation, and is also a short-lived greenhouse gas with a positive radiative forcing of 0.40 (0.20 to 0.60) W m<sup>-2</sup> (Shindell et al., 2013; Stevenson et al., 2013; Stocker et al., 2013; Cooper et al., 2014; Monks et al., 2015). Tropospheric ozone is generated through sunlight driven chemical oxidation of CO, CH<sub>4</sub>, and other non-methane volatile organic compounds (NMVOCs) in the presence of nitrogen oxides (NO<sub>x</sub>=NO+NO<sub>2</sub>). It can also be transported from the stratosphere. In October 2015, the US Environmental Protection Agency (EPA) lowered the National Ambient Air Quality Standard (NAAQS) for ozone, defined as the annual fourth-highest daily maximum 8-h average (MDA8) concentration averaged over three years, from 75 ppbv to 70 ppbv (US EPA, 2015). Attaining this lower ozone air quality standard places new challenges for the US states (Cooper et al., 2015).

Ozone over the mountainous western US (US Intermountain West), extending between the Sierra Nevada/Cascades to the west and the Rocky Mountains in the east, has recently drawn an increasing attention (Cooper et al., 2015; Lin et al., 2015a). Unlike in the eastern US, where NO<sub>x</sub> emission controls have led to ozone declines, surface ozone concentrations in the Intermountain West have been increasing in the 1990-2010 period most likely caused by rising background ozone (Jaffe et al., 2007;

55 Cooper et al., 2012; Lin et al., 2015a), although recent research suggests that these trends flatten out or even reverse in the later decade (2000-2010) (Cooper et al., 2014; Simon et al., 2015; Strode et al., 2015). The North American background ozone, defined by the US EPA as the surface ozone concentration that would be present over the US in the absence of anthropogenic emissions from North America (US EPA, 2006), is particularly high in the Intermountain West due to high elevation, arid  
60 landscape, and frequent large-scale air subsidence (Fiore et al., 2002; McDonald-Buller et al., 2011; Zhang et al., 2011; Emery et al., 2012; Dolwick et al., 2015). The background ozone includes ozone contributed by anthropogenic emissions outside North America, e.g., over Asia and Europe (Zhang et al., 2009; Cooper et al., 2010; Lin et al., 2012a), as well as natural sources such as lightning (Mueller et al., 2011; Zhang et al., 2014), wildfires (Jaffe et al., 2008, 2013; Mueller et al., 2011; Zhang et al.,  
65 2014), and stratospheric influxes (Lin et al., 2012b, 2015b; Zhang et al., 2014). A number of studies have shown that model simulations considering rising Asian emissions and global methane can only explain part of the observed increasing ozone trends in the western US (Fiore et al., 2009; Koumoutsaris et al., 2012; Parrish et al., 2014).

70 Wildfires are potentially important sources of background ozone, as they emit large amounts of NO<sub>x</sub>, CO, and NMVOCs particularly in summer under hot and dry weather conditions conducive to ozone formation. There is evidence that the frequency and intensity of wildfires in the western US have been



increasing from 1970s to 2005 driven by increasing temperatures and earlier snowmelt (Westerling et al., 2006). The number of high-ozone days is shown to have a strong interannual correlation with  
75 wildfire burned area over this region (Jaffe et al., 2008; Jaffe and Wigder 2012). However, quantifying ozone production in wildfire plumes is complicated by various uncertainties including those in wildfire emissions, chemical reactions, and variations in meteorology such as changes in temperature (Jaffe and Wigder 2012). Fire emissions of ozone precursors vary significantly among different ecosystem types, biomass nitrogen loads, and combustion efficiency (Andreae et al., 2001; Akagi et al., 2011). Ozone  
80 chemistry in fire plumes shows strong non-linearity with observations of ozone over CO enhancements ( $\Delta O_3/\Delta CO$ ) in fire plumes ranging from -0.1 to 0.9 ppbv ppbv<sup>-1</sup> depending on plume ages, aerosol effects, and mixing with urban emissions (Real et al., 2007; Jaffe and Wigder 2012; Singh et al., 2012; Parrington et al., 2013; Baylon et al., 2014). Previous studies also suggested that rapid conversion of  
NO<sub>x</sub> to peroxyacetyl nitrate (PAN) would limit ozone production near the fires (especially at low  
85 temperatures), but decomposition of PAN could lead to additional ozone production further downwind of the fires (Alvarado et al., 2010; Jaffe et al., 2013).

A standard approach to quantify the influence of a particular source on ozone concentrations is provided by chemical transport models (CTMs) using the differences between model simulations with  
90 and without this source. This Eulerian approach has been applied in numerous studies to examine

ozone from different sources based on global and regional CTMs (Pfister et al., 2007; Alvarado et al., 2010; Grell et al., 2011; Jiang et al., 2012; Zhang et al., 2014). However, application of this approach to assess wildfire ozone influences in the US Intermountain West is particularly challenging due to uncertainties in wildfire emissions and model chemistry as well as limited model resolution (Zhang et al., 2014). Our current understanding of wildfire influences on the variability and long-term trends of surface ozone is rather limited (Jaffe and Wigder 2012; Fiore et al., 2014).

In this study, we propose a new approach to estimate the influence of wildfires on surface ozone concentrations in the US Intermountain West. We define a Fire Index using the retroplumes (plumes of back-trajectory particles) calculated by a Lagrangian particle dispersion model (FLEXPART) combined with a daily high-resolution wildfire area burned dataset. We then develop multiple linear regression (MLR) models to estimate surface ozone concentration as a function of the Fire Index and other meteorological parameters, which allow us to separate the influences of wildfires and meteorology. We apply this approach to interpret surface ozone concentrations measured at CASTNet (the Clean Air Status and Trends Network) sites in the US Intermountain West during the summers (June, July and August) 1989-2010, and to quantify wildfire influences on the ozone interannual variability, trends, and exceedance days (MDA8 ozone > 70 ppbv) over this region. The Lagrangian-based wildfire ozone influences are also compared with those estimated by a Eulerian

model (GEOS-Chem) to evaluate the consistency and difference between the two.

110

## 2 Materials and Methods

### 2.1 Data description

We use measurements of ozone, organic carbon (OC) aerosols, meteorological parameters, and wildfire area burned data at daily temporal resolution. Hourly measurements of ozone as well as

115 meteorological parameters including surface temperature, wind speed, relative humidity (RH), and solar radiation are accessed from CASTNet, a long-term monitoring network established to assess the trends in air pollution and acid deposition due to emission regulations (<http://www.epa.gov/castnet>).

We focus on measurements at 13 CASTNet sites in the US Intermountain West for 1989-2010 (Figure 1 and Table 2). Most CASTNet sites have ozone measurements for the 22-year period except for Mesa Verde National Park (NP) (MEV), Great Basin NP (GRB), Canyonlands NP (CAN), and Big Bend NP (BBE) (since 1995), and Petrified Forest (PET) (since 2003). The Yellowstone NP (YEL) site 120 experienced monitor relocation in 1996, and we access the 1989-1995 measurements at the earlier YEL site from the National Park Service (NPS) following Jaffe et al. (2007) and Cooper et al. (2012).

125 In addition, we use hourly ozone measurements from 1990-2010 at the Salt Lake City (SLC, 40.6N, 111.9W, 1300m) urban site (data available at <https://www3.epa.gov/airdata/>) for comparison with the

CASTNet background sites and the previous work of Jaffe et al. (2013). Measurements of OC aerosol are from collocated sites of the Interagency Monitoring of Protected Visual Environments (IMPROVE, <http://vista.cira.colostate.edu/improve/>). OC aerosol concentrations are 24-hour averages measured every 3 days.

We also use the daily wildfire area burned data over North America for 1989-2010 developed by Yue et al. (2013) that has a  $0.5^{\circ} \times 0.5^{\circ}$  horizontal resolution. This inventory is constructed using the inter-agency fire reports from the national Fire and Aviation Management Web application system (FAMWEB, <https://fam.nwcg.gov/fam-web/>), and applied with a daily scaling factor for the duration of each fire event based on local meteorological variables (Yue et al., 2013). The total areas burned in the Intermountain West range from 90,000 to 2,000,000 hectares (ha) in the summers 1989-2010 with a large spatial and interannual variability. This wildfire area burned inventory has been used in Zhang et al. (2014) and was able to capture the episodic enhancements of OC aerosol concentrations measured in the Intermountain West for the summers 2006-2008.

## **2.2 Fire Index calculation with the FLEXPART model**

Jaffe et al. (2008) previously identified the impacts of wildfires on ozone at a measurement site using values of monthly wildfire area burned or carbon burned within a certain region around the site (e.g.,

145 10°×10° or 5°×5°). This fire indicator generally ignores the variable influence of transport of fire plumes to the site. For instance, a fire downwind of the measurement site, even one burning in the immediate vicinity, would not influence the site. Here we propose a new fire indicator using 5-day retroplumes simulated by the FLEXPART Lagrangian particle dispersion model and the daily wildfire area burned inventory mentioned above. A retroplume consists of a large number of back trajectory  
150 particles that are released from a particular receptor location (Cooper et al., 2005). We use FLEXPART version 8.02, which is first described by Stohl et al. (2005) and has been applied to examine transport of ozone (Cooper et al., 2010) and radionuclides across the Pacific Ocean (Stohl et al., 2012). FLEXPART simulates the long-range and mesoscale transport, diffusion, dry and wet deposition of gases or particles (Stohl et al., 2005). It is driven by the National Center for  
155 Environmental Prediction (NCEP) Climate Forecast System Reanalysis (CFSR) data with 1-hour temporal resolution, 0.5°×0.5° horizontal resolution, and 37 vertical levels extending from the surface to 1 hPa.

For each day at a receptor site, FLEXPART was run in backward mode, with 250,000 particles  
160 released at the site location at a constant hourly rate (~10k particles per hour) during the first 24 hours. Previous studies have used the particle sizes of 40000 (Cooper et al., 2010) and 1 million (Stohl et al., 2012) represent a retroplume. Each particle carries a small amount of mass decaying with an e-folding

time of 5 days (mean lifetime of ozone in the Intermountain West due to chemical loss and dry deposition as shown in Fiore et al. (2002)). Trajectories of these particles are calculated backwards for  
165 5 days (120 hours), together tracing the retroplume of the air arriving at the site. The model outputs are in the same  $0.5^\circ \times 0.5^\circ$  horizontal resolution as the wildfire area burned data, and are hourly residence times of the particles in each grid cell. The residence time provides a quantitative measure of the sensitivity of the simulated mixing ratio at the site location to emission input (Stohl et al., 2003; Seibert and Frank, 2004; Cooper et al., 2010). In total, we have computed over 28000 FLEXPART  
170 retroplumes for the 13 Intermountain West CASTNet sites and SLC site for the summers 1989-2010.

We then define a Fire Index (FI) as the product of daily FLEXPART residence time integrated from the surface to 5 km and daily wildfire area burned, in unit of  $s \cdot ha$ . We use 5 km in the vertical because previous studies have shown that fire emissions are occasionally lifted to above the planetary boundary  
175 layer up to 5 km above the surface (Val Martin et al., 2010; Sofiev et al., 2013), and as shown in Table S1, it provides slightly better correlations with the OC aerosol concentrations than values with 2 km and 2-4 days. The sum of Fire Index over the 5-day period is defined as Total Fire Index (TFI). The formulas are given as:

$$FI(n) = \sum_i \sum_j E_{\text{fire}(i,j,n)} \times t_{r(i,j,n)} \quad (1)$$

$$180 \quad TFI = \sum_{n=1}^5 FI(n) \quad (2)$$

Here  $E_{\text{fire}(i,j,n)}$  is the wildfire area burned in the model grid cell  $i$  (longitude) and  $j$  (latitude) on day  $n$ ,  $t_{r(i,j)}$  is FLEXPART calculated daily residence time as described in detail by Stohl et al. (2003) and Seibert and Frank (2004), and  $n$  defines the backward day in the 5-day period. Figure S1 shows an example of Fire Index for the site CAN on July 14, 2006. In this case, the particles are released on July 14 (day  $n=1$ ) in the FLEXPART model, and daily residence time is calculated backwards for 5 days (July 10-14). FI(5) then represents the product of residence time on July 10 and wildfire areas burned on that day. TFI as the sum of FI(1)-FI(5) estimates the total impact of wildfires during the 5 days for that site and day.

### 190 **2.3 Multiple linear regression model**

We build multiple linear regression (MLR) models of summer ozone concentrations for the 13 CASTNet sites and SLC site using Fire Index and meteorological parameters as predictors. This method has been previously used to identify the meteorological factors determining concentrations of particulate matter or ozone (Camalier et al, 2007; Tai et al., 2010, 2012; Jaffe et al., 2013). Here we use the metric of daily maximum 8-hour average (MDA8) ozone concentration, as it is the regulatory form of the NAAQS. A total of 28 meteorological parameters are considered in the MLR models including those measured at surface and from NCEP data (Table 1 and Table 2). Some of these meteorological variables, such as surface temperature, relative humidity, and upper level winds, have

been shown before to be correlated with surface ozone in the western US (Jacob et al., 2009;  
200 Rasmussen et al., 2012; Jaffe et al., 2013).

Wildfire ozone enhancements are sensitive to plume ages. As summarized in Jaffe et al. (2012),  
 $\Delta O_3/\Delta CO$  values in wildfire plumes show distinct differences for plume ages of 1-2 days (average  
0.018 ppbv/ppbv) versus 3-5 days (average 0.15 ppbv/ppbv). Thus instead of using TFI, we separate it  
205 to  $FI_s$  ( $FI(1)+FI(2)$ ) and  $FI_l$  ( $FI(3)+FI(4)+FI(5)$ ) in the MLR models. We also include the square root of  
 $FI_s$  and  $FI_l$  ( $SqrFI_s$  and  $SqrFI_l$ ) as variables in the regression model to at least partly account for the  
non-linearity of ozone chemistry in wildfire plumes, and to narrow the distribution of FI values that are  
highly episodic. We do not use the natural logarithm form of FI in MLR, because many of the FI  
values are zero that would cause invalid values in the regression.

210

The MLR models can be described as:

$$y = \alpha_1 \times FI_s + \alpha_2 \times FI_l + \beta_1 \times SqrFI_s + \beta_2 \times SqrFI_l + \sum_{p=1}^m \gamma_p \times met_p + c \quad (3)$$

Here  $y$  is MDA8 ozone concentration,  $\alpha, \beta, \gamma$  are the regression coefficients,  $met$  denotes the  $m$   
meteorological parameters included, and  $c$  is the constant term. We then estimate ozone enhancements  
215 from wildfires and we refer it as MLR wildfire ozone, following:

$$y_{\text{fire}} = \alpha_1 \times FI_s + \alpha_2 \times FI_l + \beta_1 \times SqrFI_s + \beta_2 \times SqrFI_l \quad (4)$$



The remaining components define the contribution from other variables such as meteorology and other sources:

$$y_{\text{nofire}} = \sum_{p=1}^m \gamma_p \times \text{met}_p + c \quad (5)$$

220 To further account for the nonlinear ozone response to wildfire emissions, we divide the ozone records for each site into three subsets based on their TFI values: subset with TFI=0; subsets with the lower 50% and upper 50% TFI values (with TFI=0 excluded). In this way we are able to quantify potentially different ozone drivers under high vs. low wildfire conditions. The MLR models as described above are applied to each subset.

225

Prior to performing the regression, we calculate correlations among ozone and all predictors and remove those factors that show weak correlation with ozone but strong dependence on other predictors.

To minimize the collinearity in the MLR model, we also apply the stepwise regression method, i.e., for each step the model selects the most powerful and significant ( $p < 0.05$ ) predictor explaining the

230 residual, and removes predictors with insignificant influence ( $p > 0.1$ ) (Field et al., 2009). We do not include the interaction terms to simplify the MLR models. We acknowledge that including FI and meteorological parameters while neglecting their interaction terms in the MLR models inevitably leads to some degree of collinearity. A measure of it is called tolerance (calculated as percent of variance in the predictor that cannot be accounted for by the other predictors) or variance inflation factors (VIF,

235 the inverse of tolerance), with VIF values greater than 10 suggesting a strong collinearity (Field et al.,  
2009). Our MLR models for all sites (Section 3) show tolerable VIF values (<5), supporting our  
approach described above to limit the collinearity.

#### 2.4 The GEOS-Chem model simulations

240 We further conduct GEOS-Chem model simulations to estimate wildfire ozone enhancements, and to  
compare with those from the Lagrangian and statistical approach as described above. The  
GEOS-Chem chemical transport model is driven by the GEOS-5 assimilated meteorological fields  
from the NASA Global Modeling and Assimilation Office (GMAO) (<http://www.geos-chem.org>;  
v8-02-03) (Bey et al., 2001). We use a nested version of GEOS-Chem that has  $1/2^\circ \times 2/3^\circ$  horizontal  
245 resolution over North America and adjacent oceans ( $140^\circ\text{W}$ - $40^\circ\text{W}$ ,  $10^\circ\text{N}$ - $70^\circ\text{N}$ ) and  $2^\circ \times 2.5^\circ$  over the  
rest of the world. We conduct the GEOS-Chem ozone simulations over North America for three-year  
(2006-2008) using the wildfire area burned of Yue et al. (2013). Zhang et al. (2014) has suggested that  
wildfire NO<sub>x</sub> emission factor in the standard GEOS-Chem simulation can be too high by a factor of 3.  
We thus also conduct a sensitivity simulation with a reduced wildfire NO<sub>x</sub> emission factor (from 3.0 g  
250 to 1.0 g NO per kg of dry mass burned following Zhang et al. (2014)). Wildfire ozone enhancements  
are computed as differences between the simulation with all emissions turned on and a sensitivity  
simulation with only wildfire emissions turned off.

### 3. Model evaluation

255 We first evaluate our Lagrangian-based Fire Index using its correlation to OC aerosol concentrations, as previous studies have shown that wildfires are an important source of OC aerosols in the US Intermountain West in summer (Park et al., 2007; Spraklen et al., 2007). As shown in Figure S2 and Table S1, the TFI values at each CASTNet site are positively correlated with OC aerosol concentrations measured at collocated IMPROVE sites ( $r=0.19-0.44$ ). While the TFI vs. OC correlations are not very strong, reflecting both uncertainties in the FLEXPART retroplumes and 260 influence from other OC aerosol sources, the correlations are better ( $p < 0.01$ ) than those with areas burned within  $10^\circ \times 10^\circ$  regions. We also test the correlations of OC aerosols with Fire Index calculated using trajectory residence time at lower altitudes or shorter backward time periods, and they in general show slightly weaker correlations (Table S1).

265 Table 2 summarizes the predictors included in the MLR models and their performance for each CASTNet site with more details given in Table S2. The MLR models explain 16%-59% of the variability in MDA8 ozone concentration among these sites. Figure 2 shows the comparison of measured and MLR predicted ozone concentrations for the ensemble of 13 CASTNet sites. The MLR 270 models generally reproduce the ozone measurements ( $R^2=0.60$ ). These coefficients of determination

( $R^2$ ) are comparable with, or even better than results simulated by Eulerian CTMs (e.g.,  $R^2 = 0.43$  in Zhang et al. (2014),  $R^2 = 0.25$  in Emery et al. (2012),  $R^2 = 0.48$  in Strode et al. (2015)) that have limited ability to reproduce the measured ozone variability in the Intermountain West probably due to the coarse model resolution and complex topography. However, they are lower than results from Jaffe et al. (2013) or Camalier et al. (2007) that applied the regression models on ozone concentrations at US urban and low-altitude sites.

Jaffe et al. (2013) analyzed the surface ozone concentrations measured at the SLC urban site in the western US during June-September 2000-2012, and showed that a MLR model using meteorological variables as predictors could explain 60% of the MDA8 ozone variation. Here we also applied our MLR models to MDA8 ozone concentrations at SLC in the summers 1990-2010. We find FI and meteorological variables can explain 48% of the daily MDA8 ozone variation for summers 1990-2010 (46% if meteorological variables alone are used, and 57% if September data are also considered that explains the higher correlation reported in Jaffe et al. (2013)), which is a higher value than at most of the CASTNet sites. In addition, as shown in Table 2 and Figure S3 the MLR model  $R^2$  values for higher-altitude CASTNet sites (> 2000m such as CNT, MEV, PND) are generally lower than values for lower-altitude sites (such as GLR, CHA and BBE). It appears that the MLR model performs better for US urban and low-altitude sites than for the CASTNet high-altitude background sites. This is likely

because ozone at the high-altitude CASTNet sites is more affected by regional transport from both anthropogenic and natural sources such as lightning and stratospheric ozone, and less controlled by local meteorology relative to ozone at urban or low-altitude sites.

We find that at the CASTNet sites daytime mean RH is generally the most important predictor. In the low-NO<sub>x</sub> background environment, HO<sub>x</sub> serves as a strong sink for ozone driving the correlation with water vapor concentrations (hence RH) (Doherty et al. 2013; Pusede et al., 2015). Fire impacts (FI<sub>s</sub> and FI<sub>l</sub>) are included for different sites, as would be expected by their different travel times from the frequent burning areas to the receptor sites. SqrFI often shows a higher explanatory power than FI, reflecting nonlinear ozone production from wildfire emissions.

We also acknowledge that the MLR models underestimate high ozone values especially when measured MDA8 ozone exceeds 70 ppbv (Figure2). These underestimates, however, are not likely due to model underestimates of wildfire ozone influences. We show in Figure 3 the relationships of TFI values with measured MDA8 ozone, MLR wildfire ozone enhancements, and MLR residuals to assess the model performance for the subset of high ozone days (MDA8 > 70 ppbv). The MLR model residuals for those high ozone days have little correlation with TFI, and most of the model underestimates occur when there are small fire impacts or fires not captured by the FLEXPART

retroplumes. We suggest these underestimates may be associated with other factors not included in the statistical model such as transport from Asia or California, from lightning emissions or stratosphere.

These processes could episodically produce more than 10 ppbv ozone in summer over the US

310 Intermountain West (Zhang et al., 2014).

## 4 Results

### 4.1 Consistency and difference with the Eulerian model

It is of particular value to evaluate the MLR wildfire ozone enhancements with those from the Eulerian  
315 approach. We show in Figure 4 such a comparison with the wildfire ozone enhancements estimated by  
the GEOS-Chem model in the summer 2007 when there are large wildfire emissions in Idaho. We can  
see that the GEOS-Chem model simulates a sharp gradient of wildfire influences with ozone  
enhancements greater than 20 ppbv over the Idaho and Montana burning areas, which decrease rapidly  
downwind to 0.5-3 ppbv.

320

To evaluate the MLR wildfire ozone enhancements, we separate the 13 CASTNet sites into three  
groups based on their distances to the major burning area in Idaho. As shown in Figure 4, the MLR  
and GEOS-Chem estimated wildfire ozone enhancements for all three groups are moderately  
correlated ( $r=0.34-0.48$ , statistically significant  $p < 0.05$ ), reflecting some consistency between the two

325 approaches. There are also considerable differences. We can see that GEOS-Chem simulates up to 40  
ppbv wildfire ozone enhancements for the short-distance sites, much higher than the MLR estimates  
(mean value of 3.96 ppbv versus 1.85 ppbv). A sensitivity simulation with a reduced wildfire NO<sub>x</sub>  
emission factor (from 3.0 g to 1.0 g NO per kg of dry mass burned) would decrease the GEOS-Chem  
mean ozone enhancement for the short-distance sites from 3.96 ppbv to 2.06 ppbv. On the other hand,  
330 for the long-distance sites, the GEOS-Chem wildfire ozone enhancements become substantially lower  
than MLR (0.77 ppbv versus 1.02 ppbv). We see GEOS-Chem largely overestimates wildfire ozone  
influences near the source regions but fails to capture continued ozone production in wildfire plumes  
downwind, as also pointed out by Zhang et al. (2014). It reflects the difficulties for Eulerian models  
such as GEOS-Chem to simulate wildfire ozone production due to, e.g., missing short-lived VOCs  
335 (Jaffe and Wigder, 2012), inadequate PAN chemistry (Alvarado et al., 2010; Fischer et al., 2014), and  
limiting all fire emissions in the boundary layer without considering their injection heights up to the  
troposphere (Val Martin et al., 2010; Sofiev et al., 2013). The lower GEOS-Chem wildfire ozone  
estimates at those long-distance sites may be also attributed to the model difficulty in simulating ozone  
production from small-scale fires nearby. The MLR approach appears to show a more reasonable  
340 pattern.

## 4.2 Contribution of wildfires to the MDA8 ozone concentration

We use the MLR models to diagnose the influences of wildfires and other meteorological parameters on MDA8 ozone concentrations at the Intermountain West CASTNet sites. Figure 5 shows the scatter-plots of observed MDA8 ozone and MLR predicted ozone at four selected sites located in different regions (GLR, ROM, GRB, and CHA). Also shown are the boxplots of MLR wildfire ozone enhancements and MLR no wildfire ozone as defined by Equation (4) and (5), respectively. The MLR models generally reproduce the measurements except for high ozone values as we have discussed above. For all the CASTNet sites, the MLR no wildfire ozone explains most of the measured MDA8 variability ( $R^2=0.10-0.58$ ) compared to MLR wildfire ozone enhancements ( $R^2=0.02-0.12$ ). However, wildfire ozone enhancements increase as measured MDA8 ozone concentrations increase, reflecting higher wildfire impacts on the high-ozone events. We can see in a few cases wildfire ozone enhancements reach 10-20 ppbv, causing measured MDA8 ozone to approach the ozone quality standard of 70 ppbv.

Another test to separate wildfire ozone influences from meteorological impacts follows Jaffe et al. (2008) who showed ozone concentrations in high-fire years were distinctly greater than those in low-fire years at the same temperature ranges. Here we extend their approach to other meteorological parameters and to the whole 22-year records. Figure 6 shows the relationships between MDA8 ozone concentrations and meteorological parameters (daytime temperature, wind speed, RH, and solar



radiation flux) measured at a Chiricahua National Monument, Arizona (CHA). We compare measured MDA8 ozone concentrations with high versus low wildfire impacts (upper 33% versus lower 33% of the TFI values). Meteorological variations have some impacts on both wildfire activities and MDA8 ozone levels. High wildfire events are prone to occur with high temperature and solar radiation, low RH and wind speed, as indicated by the number of upper 33% versus lower 33% TFI occurrences in each increment of meteorological parameters. Ozone concentrations generally increase with increasing temperature and decreasing RH. We can also see significant differences ( $p < 0.05$ ) in the MDA8 ozone concentrations between the upper and lower TFI values for most of the meteorological increments. For instance, in the 26-28°C temperature bin, the mean MDA8 ozone for the upper 33% TFI is about 8 ppbv higher than that for the lower 33% TFI. This confirms impacts of wildfires on ozone that are independent from meteorological variables.

### **4.3 Wildfire influences on the ozone interannual variability and trend**

Application of the MLR models to the summers 1989-2010 ozone measurements allows us to quantify wildfire influences on the long-term ozone variability and trend. We show in Figure 7 time series of summer mean measured and MLR predicted MDA8 ozone concentration for the Intermountain West regional average, as well as for three individual sites (GLR, YEL, and GRC) in the 22 years (1989-2010). The MLR models show good agreements with measurements with correlation

coefficients of 0.85 for the regional average and 0.52-0.92 for individual sites, but underestimate the  
380 measured interannual variability. Figure 7 also shows the summer mean MLR with and without the  
wildfire ozone, along with the difference between the two. The interannual variability of surface ozone  
over the region appears to be more controlled by the interannual variations of meteorological  
parameters, and hence the climate variability, as we can see that even without wildfire influences, the  
remaining meteorological parameters used in the MLR models still predict most of the interannual  
385 variability (MLR no wildfire ozone vs. MLR ozone  $r = 0.87-0.99$  among individual sites). This is  
further supported by the strong interannual correlations between summer mean MDA8 ozone and  
meteorological parameters such as daytime mean RH and surface temperature at individual sites and  
for the regional averages ( $r = -0.69$  for RH,  $r = 0.48$  for temperature), as shown in Figure S4.

390 Wildfires contribute 0.3-1.5 ppbv to the summer mean surface MDA8 ozone averaged over the  
Intermountain West CASTNet sites. In the high-fire activity years such as 2003 and 2007, the summer  
mean wildfire ozone enhancements can reach 3.5 ppbv at the individual sites, e.g., MEV. The  
interannual variability of wildfire ozone enhancements is strongly correlated with that of the MLR  
total ozone ( $r = 0.89$  for the regional averages and 0.48-0.87 for individual sites). As we can see here,  
395 the wildfire-driven interannual variability (0.3-1.5 ppbv) is much weaker than what can be explained  
by meteorological parameters (49.4-53.5 ppbv for the regional averaged MLR no wildfire ozone). We

suggest that some of the strong correlation between summer mean surface ozone concentrations and wildfire activities reflects their common relationships with meteorological parameters such as RH and temperature at the interannual scale, e.g., hot and dry summers would have higher ozone concentrations due to stronger photochemistry as well as more wildfire emissions than cold and wet summers (Figure S4). However we should acknowledge that ozone production in wildfires varies significantly (Jaffe and Wigder 2012), and the statistical models we use here can still underestimate the interannual variations of wildfire influences. Better resolving the causes of variations in wildfire ozone production will help us understand the source for interannual variations in ozone.

405

We further calculate the linear trends of surface ozone in the summers 1989-2010. Figure 8 summarizes the results at three percentile ranges: 93-97<sup>th</sup>, 48-52<sup>th</sup>, 3-7<sup>th</sup> percentiles at the Intermountain West CASTNet sites. The three percentile ranges are used to quantify trends in the low, median, and high windows of summer MDA8 ozone concentration. They also allow us to properly calculate the corresponding mean wildfire ozone contributions to total ozone by using percentile ranges rather than a single percentile. We find similar results when using other percentile ranges (49-51<sup>th</sup> or 47-53<sup>th</sup>). We also show the separated trends for the earlier (1989-1999) and later (2000-2010) periods following Strode et al. (2015) who suggested different trends in surface ozone for the two periods. Regional averaged summer MDA8 ozone concentrations in the Intermountain West

415 show increasing but statistically insignificant trends of  $0.14 \pm 0.21$  ( $p=0.22$ ),  $0.19 \pm 0.21$  ( $p=0.08$ ), and  
0.18 $\pm$ 0.20 ( $p=0.09$ ) ppbv year<sup>-1</sup> at the 93-97<sup>th</sup>, 48-52<sup>th</sup>, and 3-7<sup>th</sup> percentiles, respectively, in  
1989-2010. Statistically significant ( $p<0.05$ ) increasing trends are found at the YEL ( $0.42 \pm 0.30$  ppbv  
year<sup>-1</sup>) and ROM ( $0.43 \pm 0.39$  ppbv year<sup>-1</sup>) sites at the median percentiles. These increasing trends  
primarily occurred in the earlier period (1989-1999), while nearly all sites show decreasing ozone  
420 trends during 2000-2010. Strode et al. (2015) attributed the earlier increasing trends to meteorological  
variations and the later decreasing trends to domestic emission controls. Our results are consistent with  
previous studies of Cooper et al. (2012) and Strode et al. (2015) who analyzed the ozone trends using  
the same CASTNet measurements but using the metric of daytime ozone concentration.

425 Also shown in Figure 8 are the corresponding ozone trends contributed by wildfires as estimated by  
the MLR models. A distinct feature is that the trends of wildfire ozone enhancements are relatively  
small but generally in the same directions as the observed ozone trends. This feature can also result  
from meteorological variations that modulate surface ozone concentrations and wildfires in similar  
directions. Most of the sites show increasing wildfire ozone in the first 11 years (1989-1999), and  
430 switch to decreases in the next 11 years (2000-2010), but only a few of them are statistically  
significant. Wildfire ozone enhancements averaged over the Intermountain West CASTNet sites  
increase at rates of  $0.02 \pm 0.05$  ppbv year<sup>-1</sup> ( $p=0.48$ ),  $0.02 \pm 0.05$  ppbv year<sup>-1</sup> ( $p=0.38$ ), and  $0.03 \pm 0.03$

ppbv year<sup>-1</sup> ( $p < 0.05$ ) at the 93-97<sup>th</sup>, 48-52<sup>th</sup>, and 3-7<sup>th</sup> percentile ranges, respectively, in the summers 1989-2010. These values account for about 15% of the observed ozone trends at the same CASTNet sites, representing small but important ozone influences from wildfires.

#### 4.4 Wildfire influences on ozone exceedance days

As the ozone air quality standard becomes stricter, it is important to quantify the number of ozone exceedances caused partly by uncontrollable sources, such as wildfires. We show in Figure 9 the mean number of days with measured MDA8 ozone concentrations exceeding 75 ppbv, 70ppbv, and 65 ppbv averaged over the 13 Intermountain West CASTNet sites in the summers 1989-2010. Also shown is the corresponding number of exceedances that would be present in the absence of wildfires (estimated as measured ozone minus the MLR wildfire ozone). We find no statistically significant trends in the number of exceedances for both the measured ozone concentrations and ozone in the absence of wildfires during the summers 1989-2010.

In the years with poor air quality conditions such as 2002 and 2003, there were more than 20 days when MDA8 ozone exceeds 65 ppbv (accounting for 22% of the summer days), and about 8 days with MDA8 exceeding 70 ppbv, the current ozone air quality standard. However, if there were no wildfire emissions, the frequency of ozone exceedance days would significantly decrease. For the total

exceedance days at the 13 sites in this period, the number with MDA8 above 65 ppbv (above 70 ppbv) would decrease by 28% to 1509 days (by 31% to 474 days). This reduction is particularly important in high fire years such as 2002-2003 and 2005-2007 when one third to half of the exceedances would not occur without the fires. In total, wildfires contribute 28%, 31% and 32% of the days with MDA8 ozone  
455 exceeds 65, 70, and 75 ppbv, respectively, reflecting small changes in the relative importance of wildfire influences as lowering the air quality standard over this region.

## 5 Conclusions

In this study, we have applied a new approach based on a Lagrangian particle dispersion model  
460 (FLEXPART) and statistical models to quantify the wildfire influences on the ozone daily and interannual variability, trends, and exceedance days over the US Intermountain West in the summers 1989-2010. The recent implementation of a more stringent ozone standard (70 ppbv) in the United States also motivates the need to better understand contributions and variations of natural ozone sources such as wildfires.

465

We introduce a Fire Index (FI), a measure of wildfires' impact at a receptor site, by using 5-day FLEXPART retroplumes (plumes of back-trajectory particles) combined with a daily high-resolution wildfire area burned dataset in the Western US. The FI values are computed for each ozone

measurement day in the summers 1989-2010 for the ensemble of 13 CASTNet sites and an urban site  
470 (SLC) over the US Intermountain West. We then develop statistical MLR models that estimate MDA8  
ozone concentrations at each site as a function of FI and various meteorological variables. We show  
that the MLR models explain 60% (estimated for the ensemble of 13 CASTNet sites) of the variability  
of MDA8 ozone over the US Intermountain West (16%-59% at individual sites), which is comparable  
with results from current Eulerian CTMs ( $R^2 = 0.25-0.48$ ).

475

The MLR models allow us to diagnose the MDA8 ozone enhancements from wildfires as well as  
ozone controlled by meteorological variables. We compare wildfire ozone enhancements estimated by  
the MLR models with those from the GEOS-Chem CTM for summer 2007. While some consistency is  
found as reflected by their moderate correlations ( $r=0.34-0.48$ , statistically significant  $p < 0.05$ ), the  
480 two methods show rather different patterns. The MLR method appears to better capture wildfire ozone  
influences at larger distances downwind of the fires or ozone produced from small-scale fires. We find  
that wildfire ozone enhancements estimated by the MLR models occasionally reach 10-20 ppbv at the  
Intermountain West CASTNet sites, and they tend to increase as measured ozone concentrations  
increase, reflecting higher wildfire impacts on the high-ozone days. Meteorological variations also  
485 show distinct impacts on both wildfire activities and MDA8 ozone concentrations. High wildfire  
events and high ozone days are often associated with high temperatures and strong solar radiation, and

low RH and wind speed.

We find wildfires increase the summer mean MDA8 ozone concentrations by 0.3-1.5 ppbv averaged  
490 over the Intermountain West CASTNet sites during 1989-2010. While the interannual variability of  
summer mean wildfire ozone enhancements is strongly correlated with that of the MLR total ozone,  
the wildfire-driven interannual variability is much weaker than the ozone variability that can be  
explained by meteorological parameters. We suggest that the strong interannual correlation between  
summer mean ozone concentrations and wildfire activities can be partly driven by their common  
495 relationships with meteorological parameters such as RH and temperature. These common  
relationships may also be responsible for the synchronous trends of summer mean surface MDA8  
ozone concentrations and wildfire ozone enhancements for either the 1989-2010 period or two  
separated 11-year periods (1989-1999 vs. 2000-2010).

500 Wildfires thus present an important source affecting surface ozone air quality in the US Intermountain  
West. Despite small enhancements when averaged seasonally or regionally, they have notable impact  
on the occurrence of ozone exceedances, reflecting the small-scale and episodic nature of wildfire  
emissions. We show that about one third of the summer days (1989-2010) with MDA8 ozone  
exceeding 70 ppbv would not occur in the absence of wildfires. A recent study by Brey and Fischer



505 (2016) investigated fire impacts on ozone at urban sites over the contiguous US, and found that fire  
ozone influences can be even higher at locations with high NO<sub>x</sub> emissions. While we have shown that  
our Lagrangian and statistical approach provides a quantitative estimate of ozone enhancements from  
wildfires, and can be applied to analyze long-term ozone records, there are still considerable  
uncertainties in this approach from both the FLEXPART calculation and the MLR models as discussed  
510 in the text. The approach also does not consider the complexity in fire emissions and cannot probe into  
the physical and chemical processes in the fire plumes. To address this issue would require more  
detailed fire plume measurements and finer-scale modeling approaches, such as imbedding a  
plume-in-grid model in CTMs.

## 515 **Acknowledgements**

This work was supported by China's National Basic Research Program (2014CB441303), and by the  
National Natural Science Foundation of China (41475112).

**4 Figures and 2 Tables are included in the supplement related to this article.**

520

## **References**

- Akagi, S.K., Yokelson, R.J., Wiedinmyer, C., Alvarado, M.J., Reid, J.S., Karl, T., Crounse, J.D. and Wennberg, P.O.:  
Emission factors for open and domestic biomass burning for use in atmospheric models, *Atmos. Chem. Phys.*, 11,  
4039-4072, doi: 10.5194/acp-11-4039-2011, 2011.
- 525 Alvarado, M.J., Logan, J.A., Mao, J., Apel, E., Riemer, D., Blake, D., Cohen, R.C., Min, K.E., Perring, A.E., Browne,

- E.C., Wooldridge, P.J., Diskin, G.S., Sachse, G.W., Fuelberg, H., Sessions, W.R., Harrigan, D.L., Huey, G., Liao, J., Case-Hanks, A., Jimenez, J.L., Cubison, M.J., Vay, S.A., Weinheimer, A.J., Knapp, D.J., Montzka, D.D., Flocke, F.M., Pollack, I.B., Wennberg, P.O., Kurten, A., Crouse, J., Clair, J.M.S., Wisthaler, A., Mikoviny, T., Yantosca, R.M., Carouge, C.C. and Le Sager, P.: Nitrogen oxides and PAN in plumes from boreal fires during ARCTAS-B and their impact on ozone: an integrated analysis of aircraft and satellite observations, *Atmos. Chem. Phys.*, 10, 9739-9760, doi: 10.5194/acp-10-9739-2010, 2010.
- 530 Andrae M.O., Merlet P.: Emission of trace gases and aerosols from biomass burning, *Global Biogeochem. Cy.*, 15, 955-966, doi: 10.1029/2000GB001382, 2001.
- Baylon, P., Jaffe, D.A., Wigder, N.L., Gao, H. and Hee, J.: Ozone enhancement in western US wildfire plumes at the Mt. Bachelor Observatory: The role of NO<sub>x</sub>, *Atmos. Environ.*, doi: 10.1016/j.atmosenv.2014.09.013, 2014.
- 535 Bey, I., Jacob, D.J., Yantosca, R.M., Logan, J.A., Field, B.D., Fiore, A.M., Li, Q., Liu, H.Y., Mickley, L.J. and Schultz, M.G.: Global modeling of tropospheric chemistry with assimilated meteorology: Model description and evaluation, *Journal of Geophysical Research: Atmospheres*, 106, 23073-23095, doi: 10.1029/2001JD000807, 2001.
- 540 Brey, S. J., Fischer, E. V.: Smoke in the City: How Often and Where Does Smoke Impact Summertime Ozone in the United States?, *Environ. Sci. Technol.*, 50, 1288-1294, doi: 10.1021/acs.est.5b05218, 2016.
- Camalier, L., Cox, W. and Dolwick, P.: The effects of meteorology on ozone in urban areas and their use in assessing ozone trends, *Atmos. Environ.*, 41, 7127-7137, doi: 10.1016/j.atmosenv.2007.04.061, 2007.
- Cooper, O.R., Stohl, A., Eckhardt, S., Parrish D. D., Oltmans, S.J., Johnson, B. J., Ne'de'lec, P., Schmidlin, F. J., Newchurch, M. J., Kondo, Y., and Kita, K.: A springtime comparison of tropospheric ozone and transport pathways on the east and west coasts of the United States, *J. Geophys. Res.*, 110, doi: 10.1029/2004JD005183, 2005.
- 545 Cooper, O.R., Parrish, D.D., Stohl, A., Trainer, M., Nédélec, P., Thouret, V., Cammas, J.P., Oltmans, S.J., Johnson, B.J., Tarasick, D., Leblanc, T., McDermid, I.S., Jaffe, D., Gao, R., Stith, J., Ryerson, T., Aikin, K., Campos, T., Weinheimer, A. and Avery, M.A.: Increasing springtime ozone mixing ratios in the free troposphere over western North America, *Nature*, 463, 344-348, doi: 10.1038/nature08708, 2010.
- 550 Cooper, O.R., Gao, R., Tarasick, D., Leblanc, T. and Sweeney, C.: Long-term ozone trends at rural ozone monitoring sites across the United States, 1990-2010, *Journal of Geophysical Research: Atmospheres*, 117, doi: 10.1029/2012JD018261, 2012.
- 555 Cooper, O.R., Parrish, D.D., Ziemke, J., Balashov, N.V., Cupeiro, M., Galbally, I.E., Gilge, S., Horowitz, L., Jensen, N.R., Lamarque, J.F., Naik, V., Oltmans, S.J., Schwab, J., Shindell, D.T., Thompson, A.M., Thouret, V., Wang, Y. and Zbinden, R.M.: Global distribution and trends of tropospheric ozone: An observation-based review, *Elementa: Science of the Anthropocene*, 2, 29, doi: 10.12952/journal.elementa.000029, 2014.
- 560 Cooper, O.R., Langford, A.O., Parrish, D.D. and Fahey, D.W.: Challenges of a lowered U.S. ozone standard, *Science*, 348, 1096-1097, doi: 10.1126/science.aaa5748, 2015.
- Doherty, R.M., Wild, O., Shindell, D.T., Zeng, G., MacKenzie, I.A., Collins, W.J., Fiore, A.M., Stevenson, D.S., Dentener, F.J., Schultz, M.G., Hess, P., Derwent, R.G. and Keating, T.J.: Impacts of climate change on surface

- ozone and intercontinental ozone pollution: A multi-model study, *Journal of Geophysical Research: Atmospheres*, 118, 3744-3763, doi: 10.1002/jgrd.50266, 2013.
- 565 Dolwick, P., Akhtar, F., Baker, K.R., Possiel, N., Simon, H. and Tonnesen, G.: Comparison of background ozone estimates over the western United States based on two separate model methodologies, *Atmos. Environ.*, 109, 282-296, doi: 10.1016/j.atmosenv.2015.01.005 , 2015.
- Emery, C., Jung, J., Downey, N., Johnson, J., Jimenez, M., Yarwood, G. and Morris, R.: Regional and global modeling estimates of policy relevant background ozone over the United States, *Atmos. Environ.*, 47, 206-217, 570 doi: 10.1016/j.atmosenv.2011.11.012 , 2012.
- Field, A.: *Discovering Statistics Using SPSS*, 3rd ed.; Sage Publications: Thousand Oaks, CA, 2009.
- Fiore, A.M., Jacob, D. J., Bey, I., Yantosca, R. M., Field, B. D., Fusco, A. C. and Wilkinson, J. G.: Background ozone over the United States in summer: Origin, trend, and contribution to pollution episodes, *J. Geophys. Res.*, 107, doi: 10.1029/2001JD000982 , 2002.
- 575 Fiore, A.M., Dentener, F.J., Wild, O., Cuvelier, C., Schultz, M.G., Hess, P., Textor, C., Schulz, M., Doherty, R.M., Horowitz, L.W., MacKenzie, I.A., Sanderson, M.G., Shindell, D.T., Stevenson, D.S., Szopa, S., Van Dingenen, R., Zeng, G., Atherton, C., Bergmann, D., Bey, I., Carmichael, G., Collins, W.J., Duncan, B.N., Faluvegi, G., Folberth, G., Gauss, M., Gong, S., Hauglustaine, D., Holloway, T., Isaksen, I.S.A., Jacob, D.J., Jonson, J.E., Kaminski, J.W., Keating, T.J., Lupu, A., Marmer, E., Montanaro, V., Park, R.J., Pitari, G., Pringle, K.J., Pyle, 580 J.A., Schroeder, S., Vivanco, M.G., Wind, P., Wojcik, G., Wu, S. and Zuber, A.: Multimodel estimates of intercontinental source-receptor relationships for ozone pollution, *J. Geophys. Res.*, 114, doi: 10.1029/2008JD010816, 2009.
- Fiore, A.M., Oberman, J.T., Lin, M.Y., Zhang, L., Clifton, O.E., Jacob, D.J., Naik, V., Horowitz, L.W., Pinto, J.P. and Milly, G.P.: Estimating North American background ozone in U.S. surface air with two independent global 585 models: Variability, uncertainties, and recommendations, *Atmos. Environ.*, 96, 284-300, doi: 10.1016/j.atmosenv.2014.07.045 , 2014.
- Grell, G., Freitas, S.R., Stuefer, M. and Fast, J.: Inclusion of biomass burning in WRF-Chem: impact of wildfires on weather forecasts, *Atmos. Chem. Phys.*, 11, 5289-5303, doi: 10.5194/acp-11-5289-2011, 2011.
- Jacob, D.J. and Winner, D.A.: Effect of climate change on air quality, *Atmos. Environ.*, 43, 51-63, doi: 590 10.1016/j.atmosenv.2008.09.051, 2009.
- Jaffe, D. and Ray, J.: Increase in surface ozone at rural sites in the western US, *Atmos. Environ.*, 41, 5452-5463, doi: 10.1016/j.atmosenv.2007.02.034, 2007.
- Jaffe, D., Chand, D., Hafner, W., Westerling, A. and Spracklen, D.: Influence of Fires on O<sub>3</sub> Concentrations in the Western U.S., *Environ. Sci. Technol.*, 42, 5885-5891, doi: 10.1021/es800084k , 2008.
- 595 Jaffe, D.A. and Wigder, N.L.: Ozone production from wildfires: A critical review, *Atmos. Environ.*, 51, 1-10, doi: 10.1016/j.atmosenv.2011.11.063, 2012.
- Jaffe, D.A., Wigder, N., Downey, N., Pfister, G., Boynard, A. and Reid, S.B.: Impact of Wildfires on Ozone Exceptional Events in the Western U.S., *Environ. Sci. Technol.*, 47, 11065-11072, doi: 10.1021/es402164f, 2013.
- Jiang, X., Wiedinmyer, C. and Carlton, A.G.: Aerosols from Fires: An Examination of the Effects on Ozone

- 600 Photochemistry in the Western United States, *Environ. Sci. Technol.*, 46, 11878-11886, doi: 10.1021/es301541k, 2012.
- Koumoutsaris, S. and Bey, I.: Can a global model reproduce observed trends in summertime surface ozone levels? *Atmos. Chem. Phys.*, 12, 6983-6998, doi: 10.5194/acp-12-6983-2012 , 2012.
- 605 Lin, M., Fiore, A.M., Horowitz, L.W., Cooper, O.R., Naik, V., Holloway, J., Johnson, B.J., Middlebrook, A.M., Oltmans, S.J., Pollack, I.B., Ryerson, T.B., Warner, J.X., Wiedinmyer, C., Wilson, J. and Wyman, B.: Transport of Asian ozone pollution into surface air over the western United States in spring, *Journal of Geophysical Research: Atmospheres*, 117, doi: 10.1029/2011JD016961 , 2012a.
- 610 Lin, M., Fiore, A.M., Cooper, O.R., Horowitz, L.W., Langford, A.O., Levy, H., Johnson, B.J., Naik, V., Oltmans, S.J. and Senff, C.J.: Springtime high surface ozone events over the western United States: Quantifying the role of stratospheric intrusions, *Journal of Geophysical Research: Atmospheres*, 117, doi: 10.1029/2012JD018151 , 2012b.
- 615 Lin, M., Horowitz, L.W., Cooper, O.R., Tarasick, D., Conley, S., Iraci, L.T., Johnson, B., Leblanc, T., Petropavlovskikh, I. and Yates, E.L.: Revisiting the evidence of increasing springtime ozone mixing ratios in the free troposphere over western North America, *Geophys. Res. Lett.*, 42, 8719-8728, doi: 10.1002/2015GL065311 , 2015a.
- Lin, M., Fiore, A.M., Horowitz, L.W., Langford, A.O., Oltmans, S.J., Tarasick, D. and Rieder, H.E.: Climate variability modulates western US ozone air quality in spring via deep stratospheric intrusions, *Nat. Commun.*, 6, 7105, doi: 10.1038/ncomms8105 , 2015b.
- 620 McDonald-Buller, E.C., Allen, D.T., Brown, N., Jacob, D.J., Jaffe, D., Kolb, C.E., Lefohn, A.S., Oltmans, S., Parrish, D.D., Yarwood, G. and Zhang, L.: Establishing Policy Relevant Background (PRB) Ozone Concentrations in the United States, *Environ. Sci. Technol.*, 45, 9484-9497, doi: 10.1021/es2022818 , 2011.
- 625 Monks, P.S., Archibald, A.T., Colette, A., Cooper, O., Coyle, M., Derwent, R., Fowler, D., Granier, C., Law, K.S., Mills, G.E., Stevenson, D.S., Tarasova, O., Thouret, V., von Schneidmesser, E., Sommariva, R., Wild, O. and Williams, M.L.: Tropospheric ozone and its precursors from the urban to the global scale from air quality to short-lived climate forcer, *Atmos. Chem. Phys.*, 15, 8889-8973, doi: 10.5194/acp-15-8889-2015 , 2015.
- Mueller, S.F. and Mallard, J.W.: Contributions of Natural Emissions to Ozone and PM<sub>2.5</sub> as Simulated by the Community Multiscale Air Quality (CMAQ) Model, *Environ. Sci. Technol.*, 45, 4817-4823, doi: 10.1021/es103645m , 2011.
- 630 Park, R.J., Jacob, D.J. and Logan, J.A.: Fire and biofuel contributions to annual mean aerosol mass concentrations in the United States, *Atmos. Environ.*, 41, 7389-7400, doi: 10.1016/j.atmosenv.2007.05.061 , 2007.
- Parrington, M., Palmer, P.I., Lewis, A.C., Lee, J.D., Rickard, A.R., Di Carlo, P., Taylor, J.W., Hopkins, J.R., Punjabi, S., Oram, D.E., Forster, G., Aruffo, E., Moller, S.J., Bauguitte, S.J.B., Allan, J.D., Coe, H. and Leigh, R.J.: Ozone photochemistry in boreal biomass burning plumes, *Atmos. Chem. Phys.*, 13, 7321-7341, doi: 10.5194/acp-13-7321-2013 , 2013.
- 635 Parrish, D.D., Lamarque, J.F., Naik, V., Horowitz, L., Shindell, D.T., Staehelin, J., Derwent, R., Cooper, O.R., Tanimoto, H., Volz-Thomas, A., Gilge, S., Scheel, H.E., Steinbacher, M. and Fröhlich, M.: Long-term changes in

- lower tropospheric baseline ozone concentrations: Comparing chemistry-climate models and observations at northern midlatitudes, *Journal of Geophysical Research: Atmospheres*, 119, 5719-5736, doi: 10.1002/2013JD021435, 2014.
- 640 Pfister, G.G., Wiedinmyer, C. and Emmons, L.K.: Impacts of the fall 2007 California wildfires on surface ozone: Integrating local observations with global model simulations, *Geophys. Res. Lett.*, 35, doi: 10.1029/2008GL034747, 2008
- Pusede, S.E., Steiner, A.L. and Cohen, R.C.: Temperature and Recent Trends in the Chemistry of Continental Surface Ozone, *Chem. Rev.*, 115, 3898-3918, doi: 10.1021/cr5006815, 2015.
- 645 Rasmussen, D.J., Fiore, A.M., Naik, V., Horowitz, L.W., McGinnis, S.J. and Schultz, M.G.: Surface ozone-temperature relationships in the eastern US: A monthly climatology for evaluating chemistry-climate models, *Atmos. Environ.*, 47, 142-153, doi: 10.1016/j.atmosenv.2011.11.021, 2012.
- Real, E., Law, K.S., Weinzierl, B., Fiebig, M., Petzold, A., Wild, O., Methven, J., Arnold, S., Stohl, A., Huntrieser, H., Roiger, A., Schlager, H., Stewart, D., Avery, M., Sachse, G., Browell, E., Ferrare, R. and Blake, D.: Processes influencing ozone levels in Alaskan forest fire plumes during long-range transport over the North Atlantic, *J. Geophys. Res.*, 112, doi: 10.1029/2006JD007576, 2007.
- 650 Seibert, P., and Frank, A.: Source-receptor matrix calculation with a Lagrangian particle dispersion model in backward mode, *Atmos. Chem. Phys.*, 4, 51-63, 2004.
- Shindell, D.T., Lamarque, J.F., Schulz, M., Flanner, M., Jiao, C., Chin, M., Young, P.J., Lee, Y.H., Rotstayn, L., Mahowald, N., Milly, G., Faluvegi, G., Balkanski, Y., Collins, W.J., Conley, A.J., Dalsoren, S., Easter, R., Ghan, S., Horowitz, L., Liu, X., Myhre, G., Nagashima, T., Naik, V., Rumbold, S.T., Skeie, R., Sudo, K., Szopa, S., Takemura, T., Voulgarakis, A., Yoon, J.H. and Lo, F.: Radiative forcing in the ACCMIP historical and future climate simulations, *Atmos. Chem. Phys.*, 13, 2939-2974, doi: 10.5194/acp-13-2939-2013, 2013.
- 655 Simon, H., Reff, A., Wells, B., Xing, J. and Frank, N.: Ozone Trends Across the United States over a Period of Decreasing NO<sub>x</sub> and VOC Emissions, *Environ. Sci. Technol.*, 49, 186-195, doi: 10.1021/es504514z, 2015.
- Singh, H.B., Cai, C., Kaduwela, A., Weinheimer, A. and Wisthaler, A.: Interactions of fire emissions and urban pollution over California: Ozone formation and air quality simulations, *Atmos. Environ.*, 56, 45-51, doi: 10.1016/j.atmosenv.2012.03.046, 2012.
- 665 Sofiev, M., Vankevich, R., Ermakova, T. and Hakkarainen, J.: Global mapping of maximum emission heights and resulting vertical profiles of wildfire emissions, *Atmos. Chem. Phys.*, 13, 7039-7052, doi: 10.5194/acp-13-7039-2013, 2013.
- Spracklen, D.V., Logan, J.A., Mickley, L.J., Park, R.J., Yevich, R., Westerling, A.L. and Jaffe, D.A.: Wildfires drive interannual variability of organic carbon aerosol in the western U.S. in summer, *Geophys. Res. Lett.*, 34, doi: 10.1029/2007GL030037, 2007.
- 670 Stevenson, D.S., Young, P.J., Naik, V., Lamarque, J.F., Shindell, D.T., Voulgarakis, A., Skeie, R.B., Dalsoren, S.B., Myhre, G., Berntsen, T.K., Folberth, G.A., Rumbold, S.T., Collins, W.J., MacKenzie, I.A., Doherty, R.M., Zeng, G., van Noije, T.P.C., Strunk, A., Bergmann, D., Cameron-Smith, P., Plummer, D.A., Strode, S.A., Horowitz, L., Lee, Y.H., Szopa, S., Sudo, K., Nagashima, T., Josse, B., Cionni, I., Righi, M., Eyring, V., Conley, A., Bowman,

- 675 K.W., Wild, O. and Archibald, A.: Tropospheric ozone changes, radiative forcing and attribution to emissions in the Atmospheric Chemistry and Climate Model Intercomparison Project (ACCMIP), *Atmos. Chem. Phys.*, 13, 3063-3085, doi: 10.5194/acp-13-3063-2013 , 2013.
- Stocker, T. F., Qin, D.; Plattner, G.-K., Tignor, M., Allen, S. K., Boschung, J., Nauels, A., Xia, Y., Bex, V., Midgley, P. M.: IPCC, 2013: Climate change 2013: The physical science basis. Contribution of working group I to the fourth assessment report of the intergovernmental panel on climate change; Cambridge University Press: Cambridge, United Kingdom and New York, NY, USA, 2013.
- 680 Stohl, A.: A backward modeling study of intercontinental pollution transport using aircraft measurements, *J. Geophys. Res.*, 108, doi: 10.1029/2002JD002862 , 2003.
- Stohl, A., Forster, C., Frank, A., Seibert, P. and Wotawa, G.: Technical note: The Lagrangian particle dispersion model FLEXPART version 6.2, *Atmos. Chem. Phys.*, 5, 2461-2474, doi: 10.5194/acp-5-2461-2005 , 2005.
- 685 Stohl, A., Seibert, P., Wotawa, G., Arnold, D., Burkhardt, J.F., Eckhardt, S., Tapia, C., Vargas, A. and Yasunari, T.J.: Xenon-133 and caesium-137 releases into the atmosphere from the Fukushima Dai-ichi nuclear power plant: determination of the source term, atmospheric dispersion, and deposition, *Atmos. Chem. Phys.*, 12, 2313-2343, doi: 10.5194/acp-12-2313-2012 , 2012.
- Strode, S.A., Rodriguez, J.M., Logan, J.A., Cooper, O.R., Witte, J.C., Lamsal, L.N., Damon, M., Van Aartsen, B., 690 Steenrod, S.D. and Strahan, S.E.: Trends and variability in surface ozone over the United States, *Journal of Geophysical Research: Atmospheres*, 120, 9020-9042, doi: 10.1002/2014JD022784 , 2015.
- Tai, A.P.K., Mickley, L.J. and Jacob, D.J.: Correlations between fine particulate matter (PM<sub>2.5</sub>) and meteorological variables in the United States: Implications for the sensitivity of PM<sub>2.5</sub> to climate change, *Atmos. Environ.*, 44, 3976-3984, doi: 10.1016/j.atmosenv.2010.06.060 , 2010.
- 695 Tai, A.P.K., Mickley, L.J., Jacob, D.J., Leibensperger, E.M., Zhang, L., Fisher, J.A. and Pye, H.O.T.: Meteorological modes of variability for fine particulate matter (PM<sub>2.5</sub>) air quality in the United States: implications for PM<sub>2.5</sub> sensitivity to climate change, *Atmos. Chem. Phys.*, 12, 3131-3145, doi: 10.5194/acp-12-3131-2012 , 2012.
- US Environmental Protection Agency, Air Quality Criteria for Ozone and Related Photochemical Oxidants (Final), Vols. I, II, and III, EPA 600/R-05/004aF-cF, 2006.
- 700 US Environmental Protection Agency, National ambient air quality standards for ozone, *Fed. Regist.*, 80, 65292-65468, 2015.
- Val Martin, M., Logan, J. A., Kahn, R. A., Leung, F.-Y., Nelson, D. L., and Diner, D. J.: Smoke injection heights from fires in North America: analysis of 5 years of satellite observations, *Atmos. Chem. Phys.*, 10, 1491–1510, doi: 10.5194/acp-10-1491-2010, 2010.
- 705 Westerling, A.L., Hidalgo, H.G., Cayan, D.R. and Swetnam, T.W.: Warming and Earlier Spring Increase Western U.S. Forest Wildfire Activity, *Science*, 313, 940-943, doi: 10.1126/science.1128834 , 2006.
- Yue, X., Mickley, L.J., Logan, J.A. and Kaplan, J.O.: Ensemble projections of wildfire activity and carbonaceous aerosol concentrations over the western United States in the mid-21st century, *Atmos. Environ.*, 77, 767-780, doi: 10.1016/j.atmosenv.2013.06.003 , 2013.
- 710 Zhang, L., Jacob, D.J., Kopacz, M., Henze, D.K., Singh, K. and Jaffe, D.A.: Intercontinental source attribution of

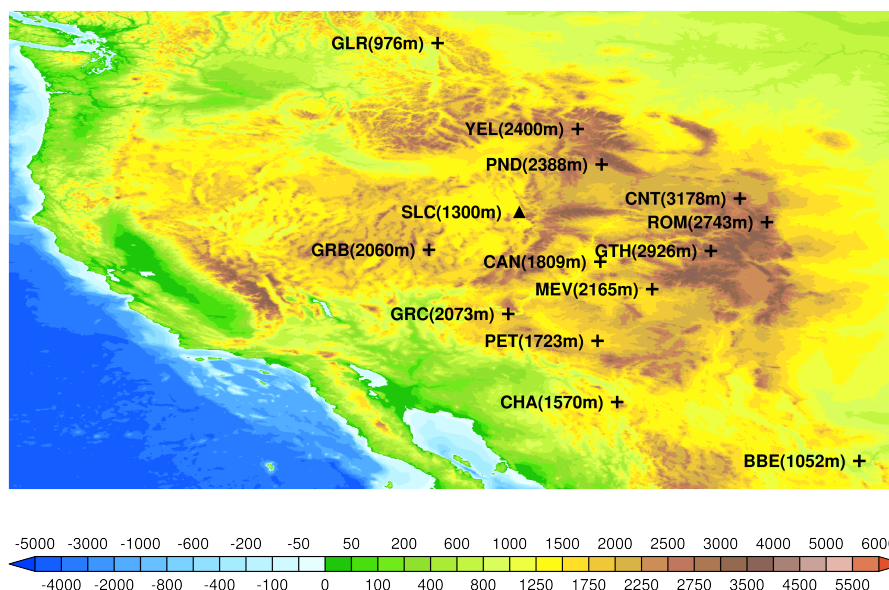
ozone pollution at western U.S. sites using an adjoint method, *Geophys. Res. Lett.*, 36, doi: 10.1029/2009GL037950, 2009.

715 Zhang, L., Jacob, D.J., Downey, N.V., Wood, D.A., Blewitt, D., Carouge, C.C., van Donkelaar, A., Jones, D.B.A., Murray, L.T. and Wang, Y.: Improved estimate of the policy-relevant background ozone in the United States using the GEOS-Chem global model with  $1/2^\circ \times 2/3^\circ$  horizontal resolution over North America, *Atmos. Environ.*, 45, 6769-6776, doi: 10.1016/j.atmosenv.2011.07.054, 2011.

Zhang, L., Jacob, D.J., Yue, X., Downey, N.V., Wood, D.A. and Blewitt, D.: Sources contributing to background surface ozone in the US Intermountain West, *Atmos. Chem. Phys.*, 14, 5295-5309, doi: 10.5194/acp-14-5295-2014, 2014.

720

## Figures and Tables



725 **Figure 1.** 13 CASTNet ozone monitoring sites (Table 2, black pluses) in the US Intermountain West  
used in this study. Also shown is SLC (Salt Lake City, Utah) urban site (filled triangle). Altitudes of  
the sites are also labeled. The underlying figure shows terrain elevations (m) of the western US.

730



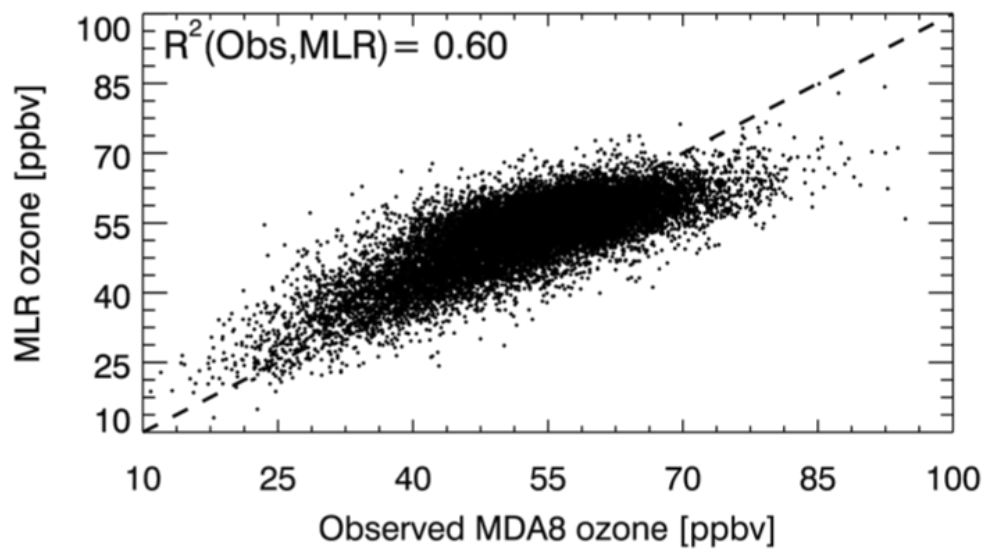
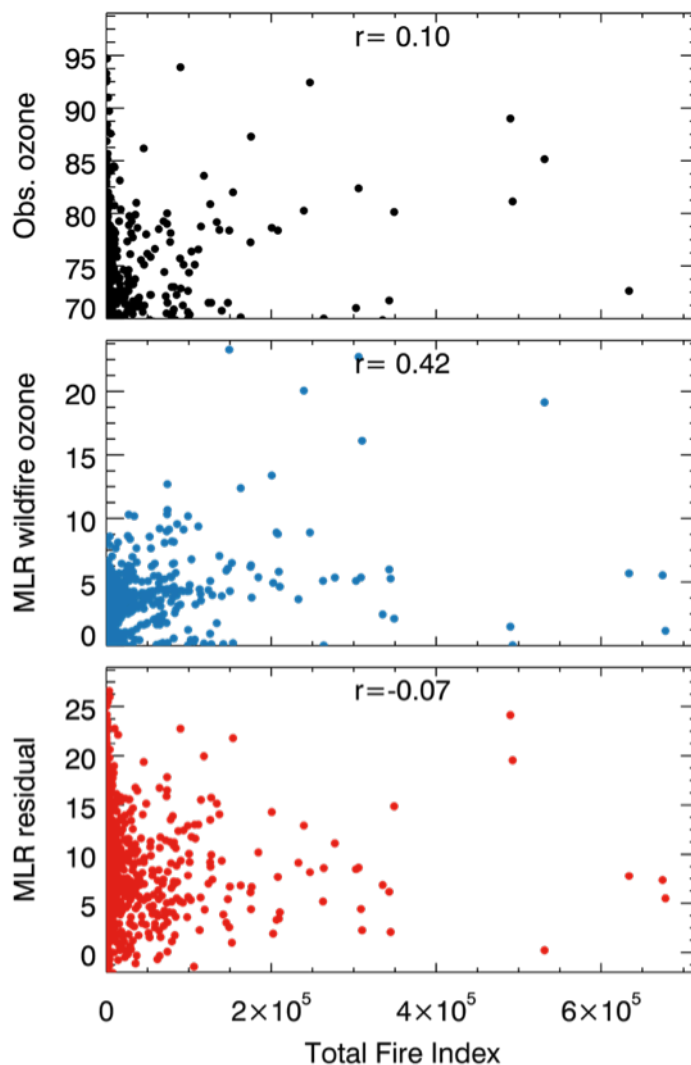
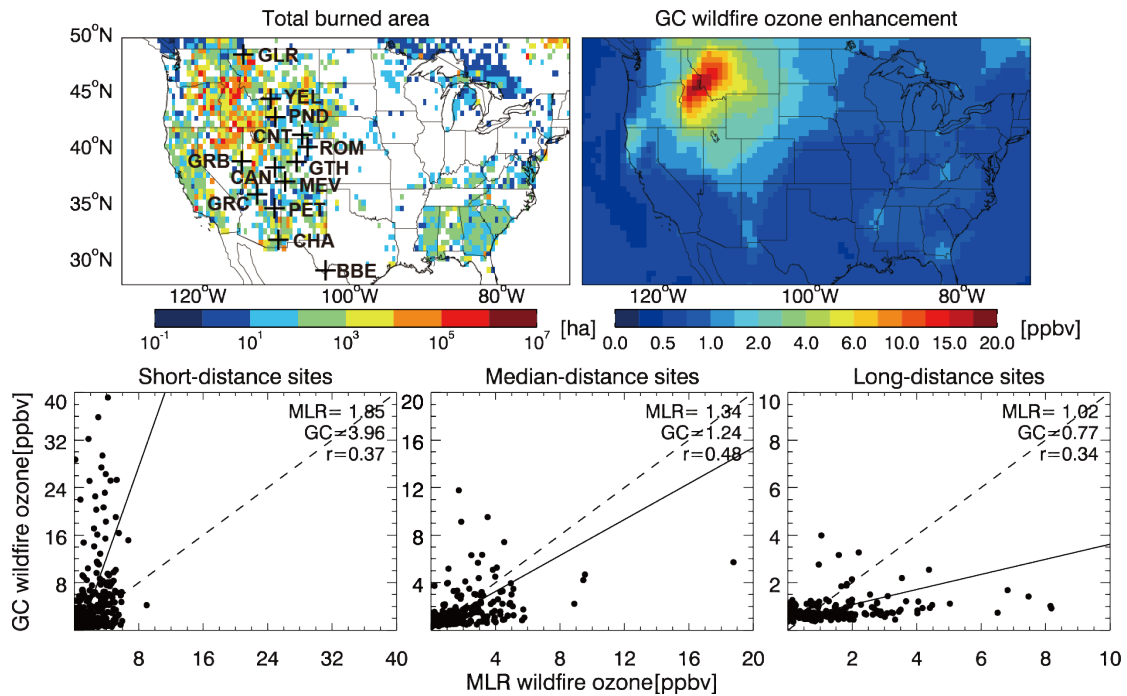


**Figure 2.** Comparison of the measured versus MLR predicted MDA8 ozone concentrations in the summers 1989-2010 for the ensemble of 13 Intermountain West CASTNet sites. The 1:1 line (dashed line) and the squared correlation are shown in the inset.



745 **Figure 3.** Evaluation of the MLR model low biases (MLR residuals) when measured MDA8 ozone concentration exceeds 70 ppbv as indicated in Figure 2. Scatter-plots of Total Fire Index (TFI) versus measured MDA8 ozone (top panel), MLR wildfire ozone enhancements (middle panel), and MLR residuals (bottom panel) are shown. The correlation coefficients are also shown inset.



750

**Figure 4.** Wildfire ozone enhancements over the Intermountain West US in summer 2007. Top panels show the total burned area (upper-left panel) and seasonal mean wildfire ozone enhancements computed by the GEOS-Chem simulation (upper-right panel). Wildfire ozone enhancements computed by the MLR models are compared with those from the GEOS-Chem simulation. The comparisons are separated by their distances to the location with the maximum fire emission in Idaho: short-distance sites (bottom-left; GLR, YEL, PND, and GRB), median-distance sites (bottom-middle; CNT, ROM, GTH, CAN, MEV, and GRC), and long-distance sites (bottom-right; PET, CHA, and BBE). Mean wildfire ozone enhancements, correlation coefficients ( $r$ ), reduced-major-axis regression lines (solid) and 1:1 lines (dashed) are shown inset.

760

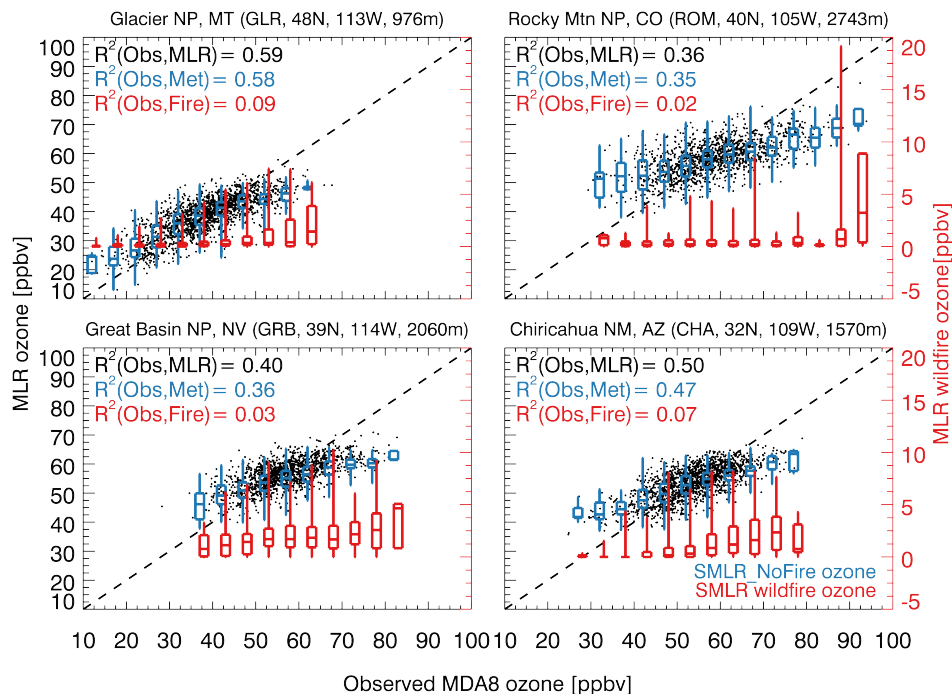
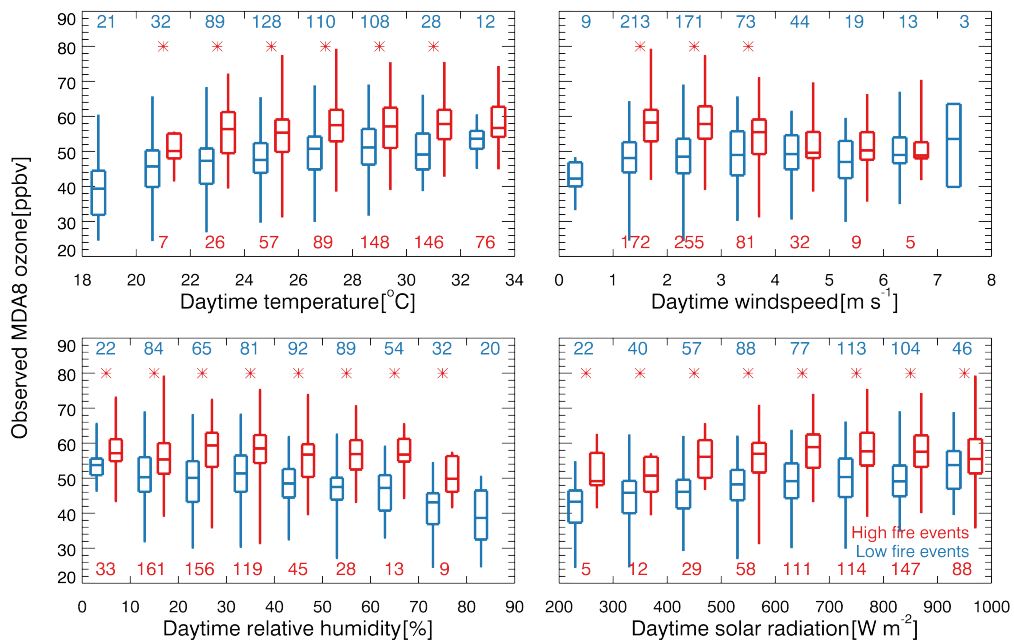


**Figure 5.** Scatter-plots of observed versus MLR predicted MDA8 ozone concentrations at 4 selected CASTNet sites for the summers 1989-2010. Also shown are the box-and-whisker plots (minimum, 25th, 50th, 75th percentile, and maximum) of ozone without wildfire influences (blue) and wildfire ozone enhancements (red) for 5-ppbv bins of observed ozone concentrations; both are computed by the MLR model as described in the text. The 1:1 line (dashed line) and the coefficient of determination ( $R^2$ ) are shown inset.



770 **Figure 6.** Box-and-whisker plots (minimum, 25th, 50th, 75th percentile, and maximum) of observed  
MDA8 ozone concentrations for bins of observed daytime meteorological parameters at CHA site:  
temperature (upper-left), wind speed (upper-right), relative humidity (bottom-left), and solar radiation  
flux (bottom-right). MDA8 ozone concentrations are divided by high (TFI at top 33%, red) and low  
(TFI at lower 33%, blue) fire events with the number of occurrences in each bin shown inset.  
775 Significant difference ( $p < 0.05$ ) is marked by asterisks.

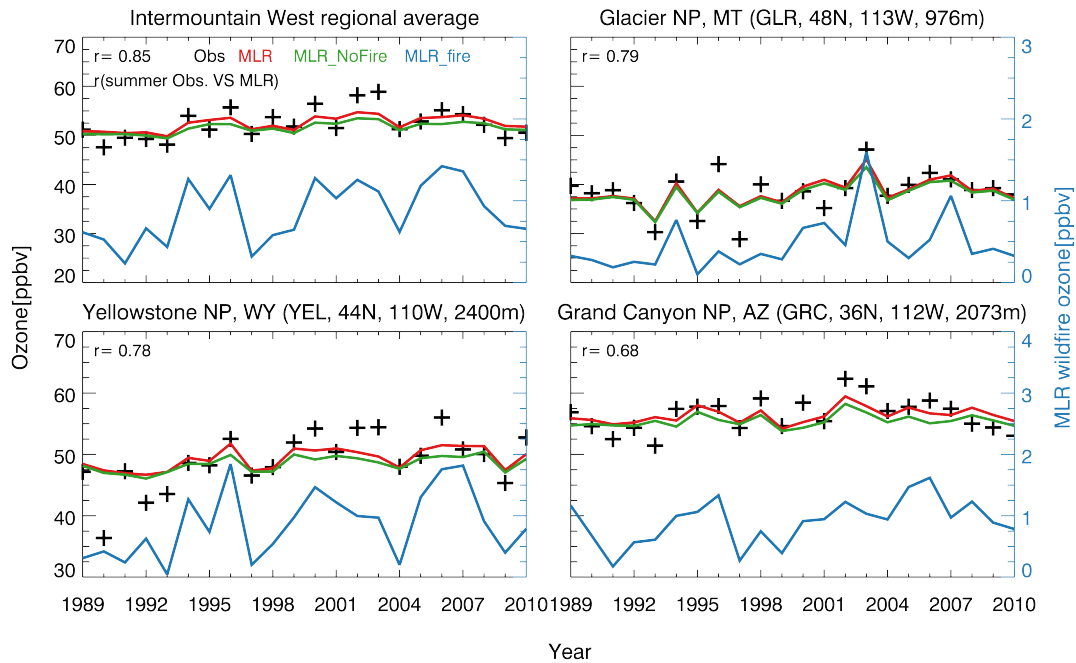
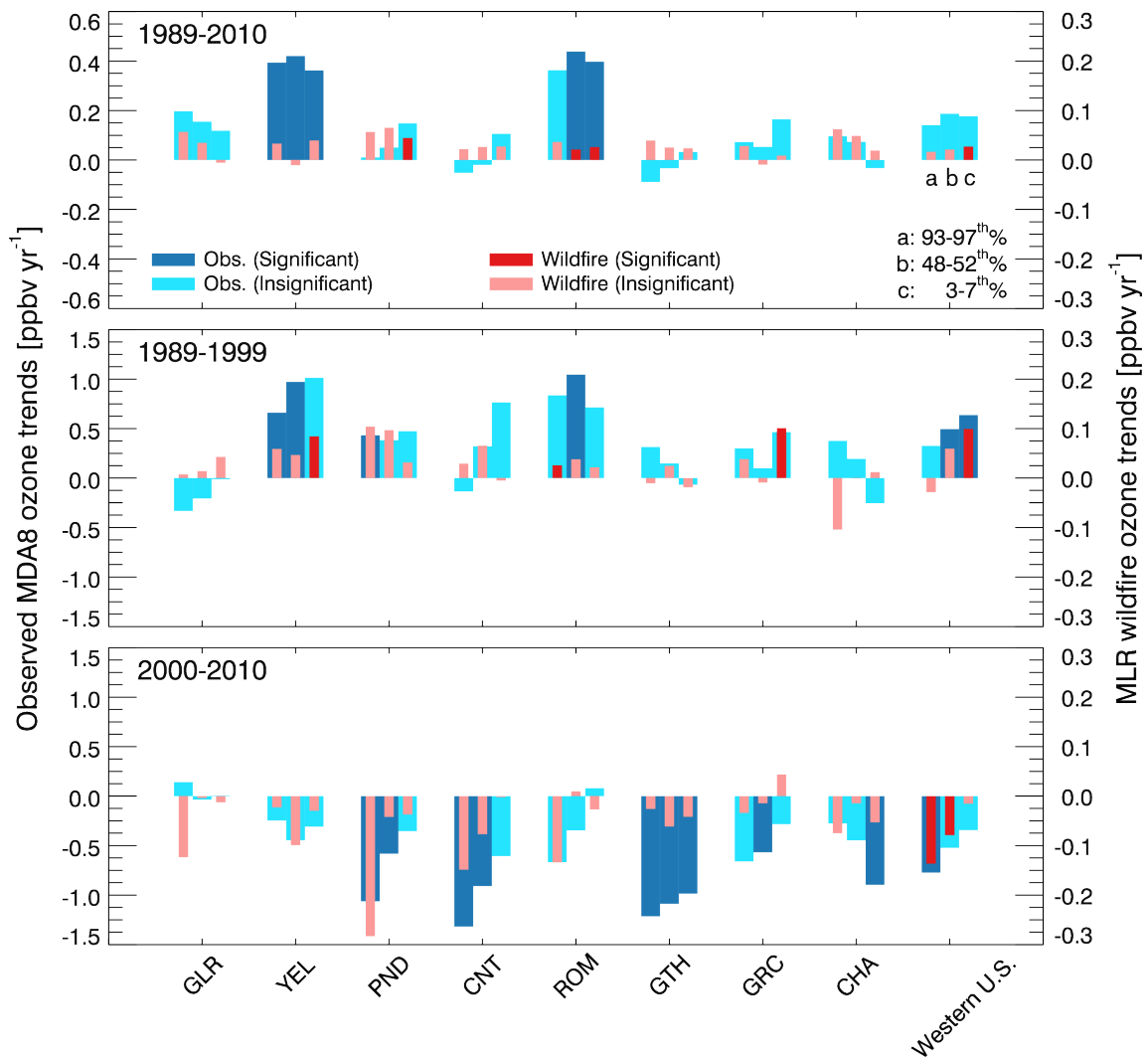


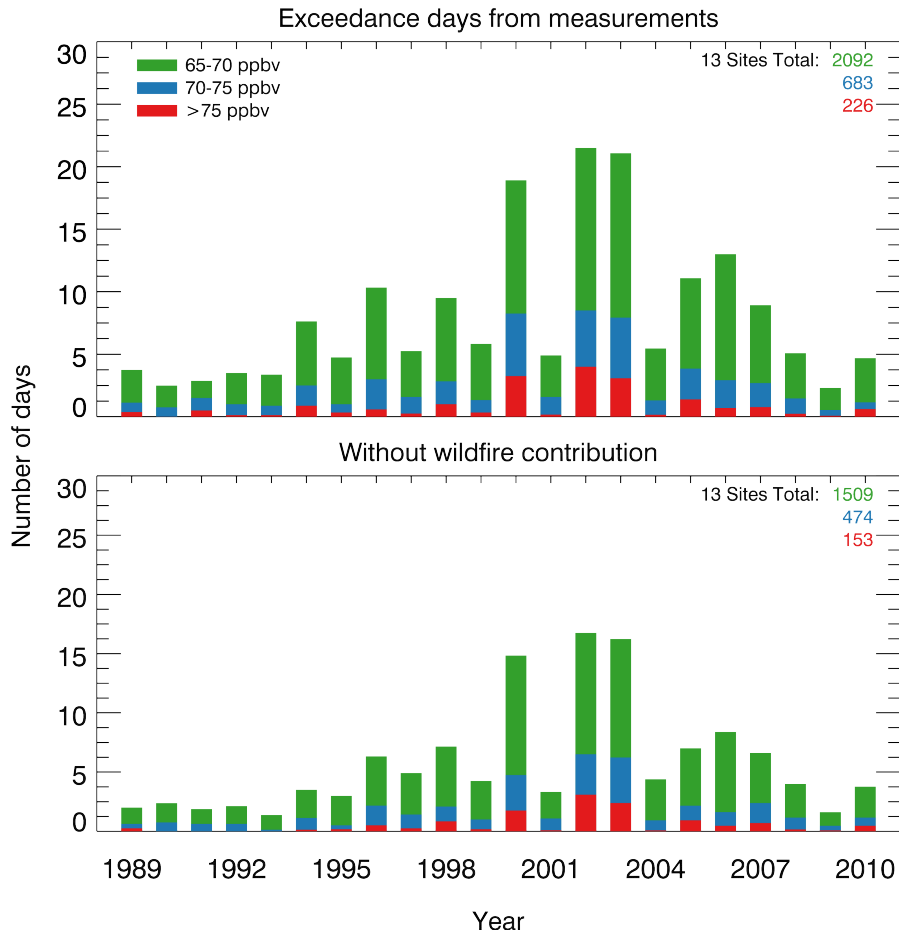
**Figure 7.** Time series of summer mean MDA8 ozone concentrations for the regional averages of 8  
780 CASTNet sites with complete 22-year measurements as well as 3 individual sites. Measurements  
(black pluses) are compared to the MLR model results (red line). Also shown are the summer mean  
MLR no wildfire ozone (green line) and MLR wildfire ozone (blue line, right axis). The correlations  
between measured and MLR summer means are shown inset.



785

**Figure 8.** Linear trends of summer mean MDA8 ozone concentrations (blue bars, left axis) for 1989-2010 (top panel), 1989-1999 (middle panel) and 2000-2010 (bottom panel) at 8 CASTNet sites and for the Intermountain West regional averages for the (a) 93<sup>th</sup>-97<sup>th</sup>, (b) 48<sup>th</sup>-52<sup>th</sup> and (c) 3-7<sup>th</sup> percentile ranges. Also shown are the trends contributed by wildfire ozone enhancements (red bars, right axis) as computed by the MLR models. Statistically significant trends ( $p < 0.05$ ) are emphasized in dark color.

790



795 **Figure 9.** Mean number of days with MDA8 ozone concentrations exceeding the thresholds of 65, 70 and 75 ppbv averaged over the 13 CASTNet sites in the Intermountain West for the summers 1989-2010. The top panel shows the exceedances computed from the measurements, and the bottom panel shows results that would be presented in the absence of wildfires (measurements minus the MLR estimated wildfire ozone enhancements).

800



**Table 1.** Variables used in the MLR models.

Variable	Predictors used in MLR model <sup>a</sup>	Data source
FI <sub>s</sub> , FI <sub>l</sub> SqrFI <sub>s</sub> SqrFI <sub>l</sub>	Fire Index for short/long period Square root of Fire Index	FLEXPART 5-day backward trajectories and 0.5°×0.5° wildfire areas burned
Tsurf WSPsurf RH SRAD	Daytime mean <sup>b</sup> surface temperature Daytime mean wind speed Daytime mean relative humidity Daytime mean solar radiation	CASTNet surface monitoring sites in the U.S. Intermountain West ( <a href="http://www.epa.gov/castnet">http://www.epa.gov/castnet</a> ), for 13 CASTNet sites only
Tmax AWND	Daily maximum temperature Daily average daily wind speed	NOAA, National Climatic Data Center: Climate Data Online ( <a href="http://www.ncdc.noaa.gov/cdo-web/">http://www.ncdc.noaa.gov/cdo-web/</a> ), for Salt Lake City urban site only
PBLH	Gridded daily maximum planetary boundary height	NCEP Climate Forecast System Reanalysis ( <a href="http://rda.ucar.edu/datasets/ds093.0/">http://rda.ucar.edu/datasets/ds093.0/</a> )
PRCP	Gridded daily precipitation	Climate Prediction Center of the National Weather Service ( <a href="ftp://ftp.cpc.ncep.noaa.gov/precip/CPC_UNI_PRCP/GAUGE_CONUS/V1.0/">ftp://ftp.cpc.ncep.noaa.gov/precip/CPC_UNI_PRCP/GAUGE_CONUS/V1.0/</a> )
U V WSP Ome SH HGT T dT	Gridded daily mean 850, 700, 500 hPa zonal wind Gridded daily mean 850, 700, 500 hPa meridional wind Gridded daily mean 850, 700, 500 hPa horizontal wind Gridded daily mean 850, 700, 500 hPa vertical velocity Gridded daily mean 850, 700, 500 hPa specific humidity Gridded daily mean 850, 700, 500 hPa geopotential heights Gridded daily mean 850, 700, 500 hPa temperature Gridded daily mean temperature at 1000mb minus that at 850 hPa	NCEP/NCAR Reanalysis dataset ( <a href="http://www.esrl.noaa.gov/psd/data/timeseries/daily/">http://www.esrl.noaa.gov/psd/data/timeseries/daily/</a> )

<sup>a</sup>Units are °C (Tsurf, T, dT, Tmax), m s<sup>-1</sup> (WSPsurf, WSP, U, V, AWND), % (RH), W m<sup>-2</sup> (SRAD), m (PBLH, HGT), kg·kg<sup>-1</sup> (SH), 0.1 mm (PRCP), and pa s<sup>-1</sup> (Ome).

<sup>b</sup>Daytime mean represents the average for 10:00-17:00 local time.

10 **Table 2.** Multiple linear regression (MLR) models for summer MDA8 ozone at 13 Intermountain West CASTNet sites<sup>a</sup>

Sites <sup>b</sup>	R <sup>2</sup> (N)	Variables included in the MLR model <sup>c</sup>
<b>Glacier NP, MT</b> (GLR, 48N, 113W, 976m)	0.59 (1809)	RH, WSPsurf, SRAD, U, V, Ome, SH, HGT, T, dT, SH, SqrFI <sub>l</sub> , SqrFI <sub>s</sub> ,
<b>Yellowstone NP, WY</b> (YEL, 44N, 110W, 2400m)	0.35 (1611)	RH, WSPsurf, Tsurf, SRAD, U, V, WSP, OME, HGT, T, dT, SH, SqrFI <sub>l</sub> , SqrFI <sub>s</sub> , FI <sub>l</sub> ,
<b>Pinedale, WY</b> (PND, 42N, 109W, 2388m)	0.28 (1888)	RH, WSPsurf, Tsurf, SRAD, U, V, WSP, Ome, HGT, T, SH, SqrFI <sub>l</sub> , SqrFI <sub>s</sub> , FI <sub>s</sub> ,
<b>Centennial, WY</b> (CNT, 41N, 106W, 3178m)	0.19 (1925)	RH, U, WSP, HGT, T, SH, SqrFI <sub>l</sub> , SqrFI <sub>s</sub> , FI <sub>s</sub> ,
<b>Rocky Mtn NP, CO</b> (ROM, 40N, 105W, 2743m)	0.36 (1367)	RH, WSPsurf, Tsurf, SRAD, PRCP, U, Ome, T, SH, FI <sub>s</sub> , SqrFI <sub>l</sub> , SqrFI <sub>s</sub> ,
<b>Gothic, CO</b> (GTH, 38N, 106W, 2926m)	0.29 (1906)	RH, WSPsurf, U, V, WSP, Ome, HGT, T, dT, SH, SqrFI <sub>l</sub> , FI <sub>l</sub> ,
<b>Mesa Verde NP, CO</b> (MEV, 37N, 108W, 2165m)	0.23 (1321)	RH, WSPsurf, Tsurf, SRAD, U, V, T, dT, SqrFI <sub>l</sub> , SqrFI <sub>s</sub> ,
<b>Great Basin NP, NV</b> (GRB, 39N, 114W, 2060m)	0.40 (1360)	WSPsurf, Tsurf, SRAD, U, WSP, Ome, SH, Ome, HGT, SH, SqrFI <sub>l</sub> , SqrFI <sub>s</sub> , FI <sub>s</sub> ,
<b>Canyonlands NP, UT</b> (CAN, 38N, 109W, 1809m)	0.16 (1379)	RH, WSPsurf, Tsurf, V, Ome, T, FI <sub>l</sub> , SqrFI <sub>l</sub> , SqrFI <sub>s</sub> ,
<b>Grand Canyon NP, AZ</b> (GRC, 36N, 112W, 2073m)	0.34 (1912)	RH, WSPsurf, SRAD, PRCP, U, V, WSP, Ome, HGT, T, SH, SqrFI <sub>l</sub> , FI <sub>l</sub> ,
<b>Petrified Forest, AZ</b> (PET, 34N, 109W, 1723m)	0.43 (654)	RH, SRAD, V, WSP, Ome, HGT, T, dT, SH, SqrFI <sub>l</sub>
<b>Chiricahua NM, AZ</b> (CHA, 32N, 109W, 1570m)	0.50 (1754)	RH, SRAD, PBLH, U, V, WSP, HGT, T, dT, SH, SqrFI <sub>l</sub> , FI <sub>l</sub> ,
<b>Big Bend NP, TX</b> (BBE, 29N, 103W, 1052m)	0.46 (1196)	RH, WSPsurf, SRAD, U, V, WSP, HGT, T, SqrFI <sub>l</sub> , SqrFI <sub>s</sub> , FI <sub>l</sub> , FI <sub>s</sub> ,

<sup>a</sup> Coefficients of determination (R<sup>2</sup>), sample numbers (N), and variables included in the MLR models.

<sup>b</sup> NP = National Park, NM = National Monument, MT = Montana, WY = Wyoming, CO = Colorado, NV= Nevada, UT = Utah, AZ = Arizona, TX = Texas.

15 <sup>c</sup> Fire Index (FI<sub>l</sub>, FI<sub>s</sub>), square root of FI (SqrFI<sub>l</sub>, SqrFI<sub>s</sub>), and meteorological parameters including (1) surface measurements: daytime (10:00-17:00 local time) mean temperature (Tsurf), wind speed (WSPsurf), relative humidity (RH), and solar radiation flux (SRAD); (2) gridded daily precipitation (PRCP); (3) NCEP data at 850/700/500 hPa pressure levels: daily maximum planetary boundary layer height (PBLH), daily mean zonal wind speed (U), meridional wind speed (V), horizontal wind speed (WSP), temperature(T), geopotential height (HGT), vertical velocity (Ome), specific humidity (SH), and temperature at 1000hPa minus that at 850 hPa (dT). Please refer to Table S1 and S3 for details on the parameters and MLR models.